Desalination and Water Treatment
www.deswater.com

doi: 10.5004/dwt.2021.26700

214 (2021) 286–293
February

Energy efficiency of polyimide membrane modules for air separation in zero-emission power plants: a computational analysis

Grzegorz Wiciak*, Krzysztof Grzywnowicz, Leszek Remiorz, Katarzyna Janusz-Szymańska

Silesian University of Technology, Faculty of Energy and Environmental Engineering, Gliwice, Poland, email: grzegorz.wiciak@polsl.pl (G. Wiciak)

Received 1 May 2020; Accepted 8 August 2020

ABSTRACT

A fundamental part of oxy-combustion zero-emission power plants is the ambient air separation unit. Amongst the various technologies utilized to perform this process, membrane gas separation might be applied as well. This paper is a continuation of previous research on operation of polyimide membranes in such power units. The presented results of computational analysis are based on experimental research, regarding the energy-related parameters of the nitrogen/oxygen separation from ambient air using commercial capillary polymer membranes. Empirical, continuous functions describe the variability of the essential parameters for membrane separation modules of variable configuration and are used as a fundamental part of the model, used within the presented research. Energy consumption and efficiency of the air separation unit are investigated as the most influencing of these parameters. Analyses are performed for three variants of unit configuration: serial connection of membrane modules, unit with retentate recirculation and unit with permeate recirculation. The results of the research indicate the essential differences in total energy consumption for the subsequent configurations. Both the highest energy demand of the air separation module, equal to 1.61 kJ/m^3 O_2, and the lowest, equal 0.02 to kJ/m^3 O_2, were obtained for the retentate recirculation (for the 800 and 1,500 L/h stream flows, respectively). Satisfactory operational parameters of the separation process were indicated for both the permeate recirculation and serial modules connection variants, with an acceptable rise in power demand, corresponding to a maximum value of 205 W and 88 W, respectively.

Keywords: Air separation; Polyimide membranes; Energy efficiency; Membrane separation unit; Zero-emission power plants

1. Introduction

Technological processes of energy generation are mainly based on the combustion of fossil fuels, such as hard coal, lignite, natural gas, or crude oil. The by-products of those processes include a series of volatile chemical compounds, including mainly: CO_2, N_2, H_2O, SO_x, and NO_x, as well as volatile organic compounds and particulate matter [1–5]. Due to the negative effects on humans (including higher risk of pulmonary and cardiovascular diseases) and the environment (by formation of acid rains and indirect water pollution by heavy metals), a number of these emissions should be separated from the stream of exhaust gases before it is released into the atmosphere [1,2,6]. Among these compounds, potentially toxic substances as well as the gaseous products of combustion, which have the greatest potential for causing global warming, might be listed [1,2,4]. Carbon dioxide and water vapor should be mentioned as the most important byproducts of the combustion process, when considering global warming [7–9].

Techniques for the production of useful energy, including electric current and heat, remain the subject of many

* Corresponding author.

1944-3994/1944-3986

profound investigations, discussed in the scientific literature [1,5,10–14], and are performed both experimentally and theoretically [1,15,16]. Worldwide energy demand is set to rise continuously, which is caused by the rapid development of markets globally. This gives rise to a higher consumption of primary energy resources, such as fossil fuels. Their extraction, processing and utilization influence not only the higher emissions of greenhouse gases – beginning with significant methane emissions from ventilation shafts [17] – but also the significant contamination of adjacent water reservoirs [18]. To limit the negative impact of fossil-based power plants and prevent further emissions, modern power generation and new technologies are indeed being introduced. Nevertheless, their widespread utilization might be limited by numerous factors [19,20].

All the processes and methods, which aim to minimize the effect of negative impacts of coal combustion on the natural environment are called clean coal technologies [21]. Following this concept, in commercial power generation units, zero-emission power plants are being introduced. Zero-emission units are characterized by the almost neutral environmental impact associated with their operation [22,23]. When considering the reduction of CO_2 emissions, these aforementioned units utilize novel technology, such as carbon capture and storage [24,25]. In order to successfully introduce such installations, three technological concepts are used: (1) pre-combustion – capturing CO_2 before the combustion of the fuel, (2) post-combustion – capturing CO_2 after the process of combustion, and (3) oxy-combustion – combustion of fuel under high oxygen concentration conditions [23,25,26].

Oxy-combustion involves the process of fuel combustion in an oxygen-enriched atmosphere, where the oxygen content is 100%. The main aim of this process is an increase in the percentage share of carbon dioxide in the total stream of exhaust gases [26,27]. The oxygen is produced in an air separation unit, where ambient air is separated into streams of oxygen and nitrogen, with some remaining residual gases [27]. Currently, to enhance its benefits, oxy-combustion technology is often mixed with other industrial combustion technologies [24]. Their main advantages are capturing carbon dioxide directly from the exhaust stream and lower energy consumption [16]. Oxygen, required to perform the process, is collected from ambient air, using several possible techniques [5,7,8].

The separation of oxygen from ambient air, using membrane methods, utilize semipermeable films (membranes) made from polymer and other materials [28,29]. Membrane separation techniques are widely applied in industrial processes, but the petrochemical industry use the techniques in the process of natural gas treatment, before further utilization [30,31]. Membranes dedicated to gas separation, in the context of energy engineering are characterized by: resistance to high temperature, chemical inertness, resistance to natural aging, possible modular connectivity and both low production and maintenance expenditure [5,28,29,32], where the introduction of these features are linked with modern material technologies. In recent research on gas separation membranes, strong emphasis has been put on searching for new polymeric or composite materials – characterized with higher permeability, selectivity and mechanical strength [33].

The membrane separation module (membrane separator) – which describes fully realized, independent device ready to be introduced within current industrial processes – is formed by a set of single membrane modules; these can connect in parallel, series, or in any combination of both. The membrane separators also include any auxiliary equipment, such as filters, compressors and measuring instruments. Separators are required to have a compact size, crucial to retrofitting existing power plants and other industrial units, as has been described in detail [34]. Furthermore, separators should be characterized by simplicity of operation and minimized number of rotating parts, resulting in reduced maintenance costs [1,16] and a possibility of improving product lifespan. The selection and type of membrane modules, dedicated for use during the construction of a given membrane separator, depends mainly on available capital expenditure and the nominal operational parameters of the unit [5,22]. Current research within the field of gas membrane separators focus on scaling the laboratory solutions and designing large-scale modules, suitable for application to industrial power plants [35,36].

The operational parameters of the separator, crucially depend upon the functioning of individual modules and therefore on the methods of module connection within the device. Apart from the parameters of the separation process, which affect fundamental applicability of a given separator and any particulars for an intended installation site, the parameters regarding economy of the solution are equally essential [5,37]. Considering the membrane separation units, maintenance costs are proportional to the internal energy demand of the unit and are a vital factor determining widespread introduction of the unit into existing plants.

This paper continues research on operational parameters of ambient air separation on polyimide membranes, discussed in the study by Remiorz et al. [24]. The aim of this article is to investigate internal power demand and energy efficiency of the oxygen/nitrogen separation process, taking place in membrane separators with variable internal module configuration and variable operational conditions. Studied configurations include: the serial connection of individual modules, multiple recirculation of the retentate and multiple recirculation of the permeate within the separator. As the variable operational condition, a feed flow rate between 700 and 1,600 L per hour has been assumed. The fundamental separation process parameters, required to calculate the energy efficiency of any individual solution, were obtained on the basis of semi-experimental research, discussed in detail in the study by Remiorz et al. [24]. The power demand has been calculated basing on a computational model of the module, following the method proposed in previous investigation [24].

2. Computational model

The computational model, used to proceed fundamental calculations on the gas separation process, is based on empirical equations. The equations are obtained on the basis of sophisticated experimental research [24] performed on a test-stand, presented in details in the study by Wiciak [38]. These resulted from mathematical analysis of experimental data regarding the operation of NM-B02A polyimide membrane, derived by UBE Industries Ltd., Japan, and selected due to its relatively wide range of operational conditions as well as relative stability in ambient air separation [24]. Discussed functions were acquired for data regarding a single-membrane module, whereas their final forms were calculated as regression functions for the highest value of the Pearson product-moment correlation coefficient [24]. The empirical equations, included within the model, characterize permeate purity Y_{O_2} (concentration of oxygen within the permeate stream) as a function of volumetric feed flow and volumetric permeate flow, according to the assumed experimental procedure discussed in the study by Remiorz et al. [24] and the presented equations (Eqs. (1) and (2)). Introduced equations were based on data for the feed pressures required to obtain stable operational conditions for the investigated membrane (equal to 11.2 and 12.2 bar, respectively – both values are within the allowable inlet pressure range of the membrane) and for feed flow varying in the range of 500–900 dm³/h – data points defined for higher flows were extrapolated, which might introduce some predictive inaccuracy. As shown in dependencies (1) and (2), double statement of the permeate purity equation was introduced to the model. To minimize the influence of individual measurement uncertainties on the computational results, as well as possible inaccuracies in respective curve fits for the working conditions of the investigated membrane, the in-time comparison and averaging of results obtained on the basis of both permeate- and feed-related equations are applied.

As the additional essential parameters, the model included experimentally obtained values of pressure decrease between the feed and the permeate, as well as the feed and the retentate, equal to 8 and 6.2 bar, respectively, at nominal conditions.

$$Y_{O_2} = -1e^{-3}Q_P^2 + 1.6795Q_P + 631.3 \tag{1}$$

$$Y_{O_2} = 9e^{-11}Q_f^4 - 3e^{-3}Q_f^3 + 4e^{-4}Q_f^2 + 162.4e^{-3}Q_f + 100 \tag{2}$$

where Y_{O_2} – permeate purity (%), Q_P – permeate volumetric flow (dm³/h), Q_f – feed volumetric flow (dm³/h).

Furthermore, part of the model included the identification of physical properties – including density, viscosity, specific enthalpy and specific entropy – of respective streams, based upon tabular datasets for the real gas model and composition. The composition of these streams is estimated using the empirical oxygen concentration dependencies (1) and (2). Based on the identified properties and empirical functions, temporary operational parameters of a given membrane module included within the separator, are investigated. Next, the respective streams are virtually added to the computational stack iteratively. Parameters of the stream, when passing through the compressors are obtained basing on energy balance, under the assumption of constant compressor efficiency. The introduced assumption is based on supposition of using a variable speed drive compressor, modulated by automatic control systems included within the separator. Such an assumption enabled implementation of single compressor data for all modeled configurations and led to both a rise in universality for the prepared model and significant reduction in computational cost. As shown in the study by Bounaceur et al. [39], to maintain satisfactory accuracy of results, effects of the Joule–Thomson expansion – which appear in the case of real piping connections between subsequent membranes – should be included within the model as well. Thus, physical properties of respective streams, virtually added to the computational stack and introduced via the energy balance calculations for any subsequent iteration, are reconsidered under isentropic expansion conditions. Simultaneously, the compressor power, required to equalize pressure of the respective streams with the pressure of both the feed and heat flow, required to maintain constant temperature, were calculated on the basis of the energy conservation equation. Finally, total energy consumed for given case and total volume of the oxygen, additionally derived by the module to the permeate, have been computed. A schematic of the computational algorithm used to obtain the results are shown in Fig. 1.

Schemes of configurations of the membrane separator, which are investigated – including: serial connection of modules, retentate recirculation and permeate recirculation – correspond to the configurations considered during the previous stage of the research, discussed in the study by Remiorz et al. [24], and are shown in Figs. 2–4, respectively.

As a result of this research, the set of characteristic parameters for the investigated separator, as well as their characteristic curves are obtained. The parameters were defined as function of the feed flow in the range of 700–1,600 dm³/h – to prevent degradation in the separation process, due to exceeding the local membrane separation capacity, ensuring efficient use of the membrane – and included:

- the permeate purity Y_{O_2},
- total power demand of compressors N_{el},

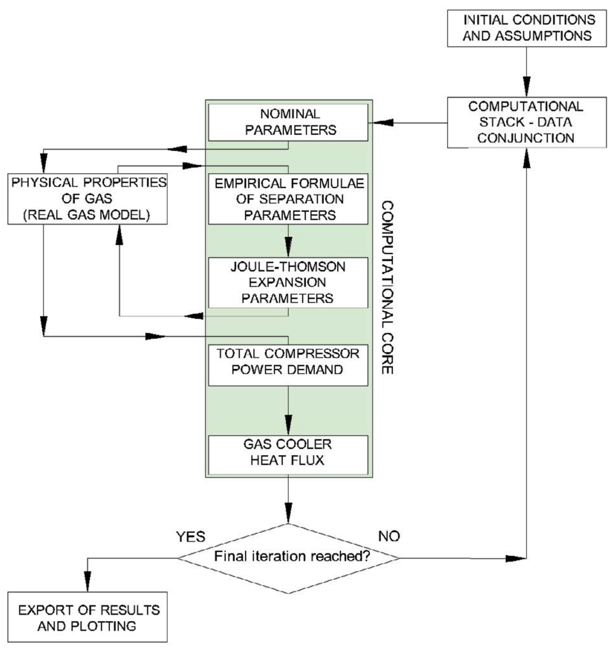

Fig. 1. Scheme of the computations performed within the applied model (based on the study by Remiorz et al. [24]).

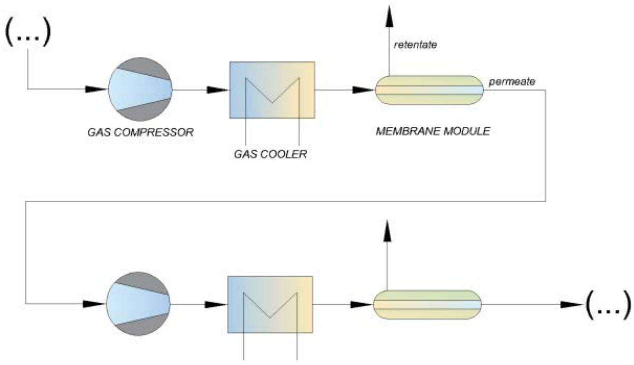

Fig. 2. Scheme of connections within the membrane separator, serial membrane connection (based on the study by Remiorz et al. [24]).

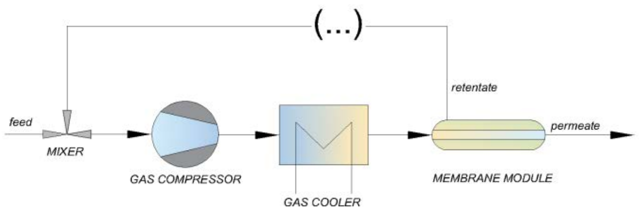

Fig. 3. Scheme of connections within the membrane separator, retentate recirculation (based on the study by Remiorz et al. [24]).

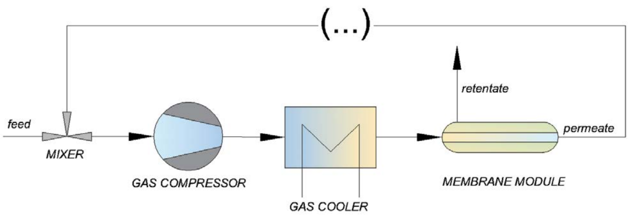

Fig. 4. Scheme of connections within the membrane separator, permeate recirculation (based on the study by Remiorz et al. [24]).

- energy efficiency of the separation N_ε, defined as energy required to enrich the permeate with 1 m^3 of pure oxygen, as indicated in Eq. (3),

$$N_\varepsilon = \frac{N_{el}}{\Delta Q_{P,O_2}} \tag{3}$$

where $\Delta Q_{P',O_2}$ – increase in the pure oxygen stream flow within the permeate.

- useful energy ratio H, defined as the ratio of total power demand of compressors to total heat flow extracted by the gas coolers, according to Eq. (4).

$$H = \frac{N_{el}}{\dot{E}_{gc}} \tag{4}$$

where $\dot{E}_{gc}$ – total heat flow extracted from gas cooler in the system.

3. Results and discussion

The first of the configurations analyzed for the proposed membrane separation unit (Fig. 2) involved the serial connection of the membrane modules by the permeate duct. In this case, the total power demand states the sum of individual demands on the subsequent inter-module compressors. The individual demands depend on the variable feed flow and the pressure drop between the feed and the permeate at nominal conditions. Results of the analysis, in terms of the characteristic power demand and power effectiveness curves, are described in Figs. 5–7.

As shown by Figs. 5–7, power consumption rises linearly with both the number of modules and feed stream flow (Fig. 5). As indicated in Fig. 6, for the serial connection of modules, the energy efficiency of the separation process N_ε does not depend on the number of modules in series. Considering the useful energy ratio H of the serial connection of modules, the power demand of the compressors corresponds to roughly 23% of thermal energy potentially extractable from gas coolers. Nevertheless, as

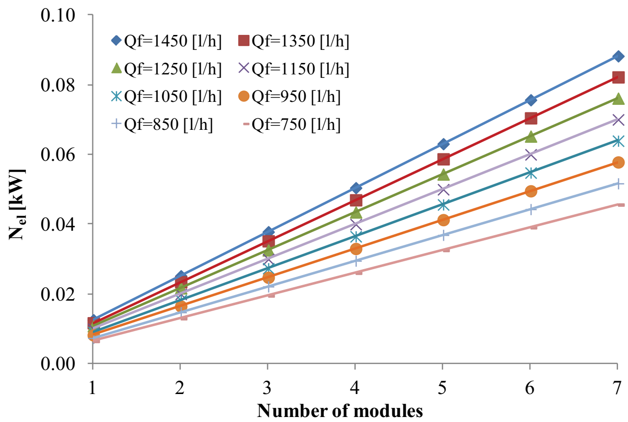

Fig. 5. Power demand of the separator, including serial connection of individual membranes, as a function of feed flow and number of modules in series.

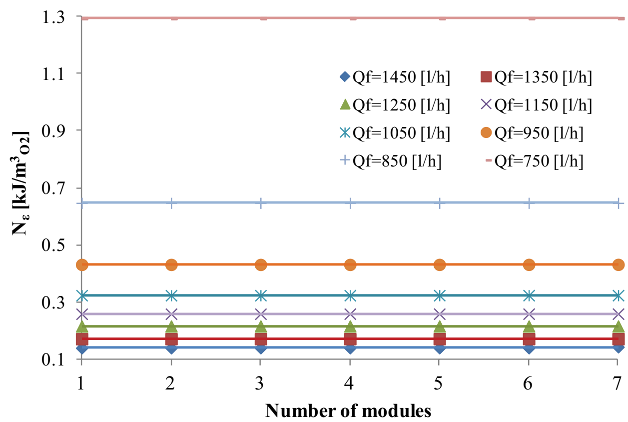

Fig. 6. Energy efficiency of the separation in the separator including serial connection of individual membranes, as a function of feed flow and number of modules in series.

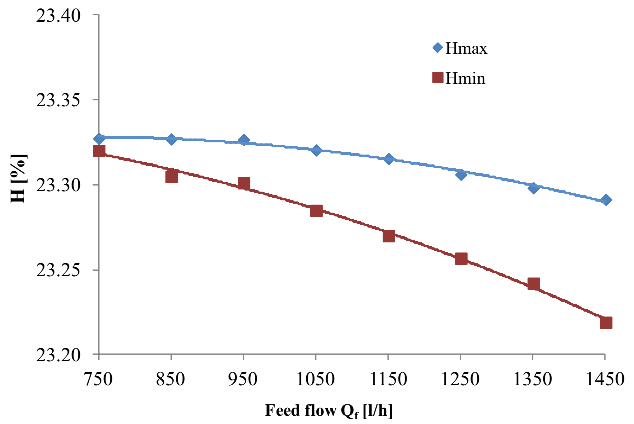

Fig. 7. Useful energy ratio of the separator including serial connection of individual membranes, as a function of feed flow and number of modules in series.

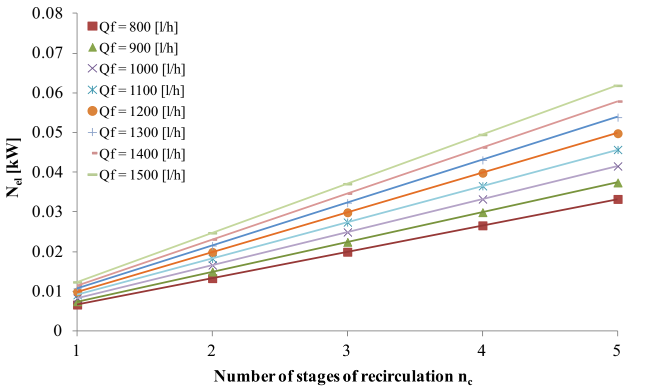

Fig. 8. Power demand of the separator including retentate recirculation, as a function of feed flow and number of retentate recirculation cycles.

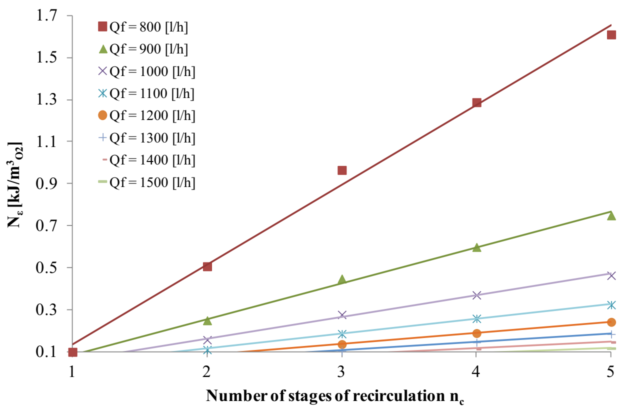

Fig. 9. Energy efficiency of the separation in the separator including retentate recirculation, as a function of feed flow and number of retentate recirculation cycles.

indicated in Fig. 7, increasing the number of individual membrane modules incorporated within a given separator, is followed by an increase in the deviation between its maximal (H_{max}) and minimal (H_{min}) values. This observation suggests that increasing the number of modules connected in series has to correspond to implementation of better process control.

The second of the investigated cases (Fig. 3) involved recirculation of the retentate and its perfect mixing with the incoming fresh feed stream. In this case, the total power demand states the sum of individual compressor demands for all subsequent portions of the feed/retentate stream, flowing through the membrane, when pressurized to the initial value. Dependence of the demand is defined by: the variable feed flow, pressure drop between the feed and the retentate at nominal conditions and each retentate stream flow being recirculated at each recirculation stage. Results are shown in Figs. 8 and 9.

Regarding Figs. 8 and 9, the power consumption curve (Fig. 8) shows good qualitative agreement with the case of serial connection of modules (Fig. 5). Nevertheless, the obtained power consumption is slightly lower than respective consumption obtained for the previously discussed case. The N_ε parameter is influenced by the feed flow Q_f, and, in contrary to the serial connection case, significantly affected by number of recirculation stages. Values of N_ε observed for the retentate recirculation (Fig. 9) are approximately 50% higher than for serial connection case (Fig. 6).

The last of the studied configurations (shown in Fig. 4) utilize multiple recirculation stages for the permeate. By analogy to the previous case, total power demand states the sum of the individual compressors demands shown for all subsequent portions of the feed/permeate stream, flowing through the membrane. The energy demand was identified as a function of the variable feed flow, nominal pressure decrease between the feed and the permeate and the permeate streams being recirculated at each stage. Results are depicted in Figs. 10 and 11.

Data depicted in Fig. 10 corresponds to the trend shown for the previously analyzed case, where the least energy demand was observed for the lowest feed stream flow, with significant dependence for individual values on both feed stream and recirculation stages. Nonetheless, the values for total power consumption are significantly higher when compared with the retentate recirculation case (up to approximately 290%). This however, cannot be inferred from the energy efficiency chart (Fig. 11) – the values of the parameter for the permeate recirculation are approximately 45% lower than for the retentate recirculation case (Fig. 9).

Data plotted in the respective figures indicate that the lowest power demand is observed for the configuration with retentate recirculation, whereas the greatest demand corresponds to the permeate configuration. For all investigated cases, the power demand N_{el} increases proportionally with increasing feed flow. This dependence comes from the accumulation of power required to compress subsequent streams either within each of the compressors used, or a single compressor for the recirculation variants. Nevertheless, considering the energy efficiency of separation N_ε, increased volumetric feed flow resulted in an essential drop of the N_ε parameter for all simulated configurations. This observation suggests that the investigated membrane requires greater pressure at the feed, in order to overcome

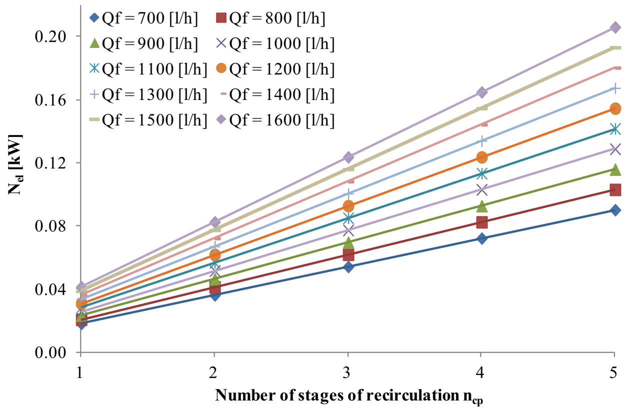

Fig. 10. Power demand of the separator including permeate recirculation, as a function of feed flow and number of permeate recirculation cycles.

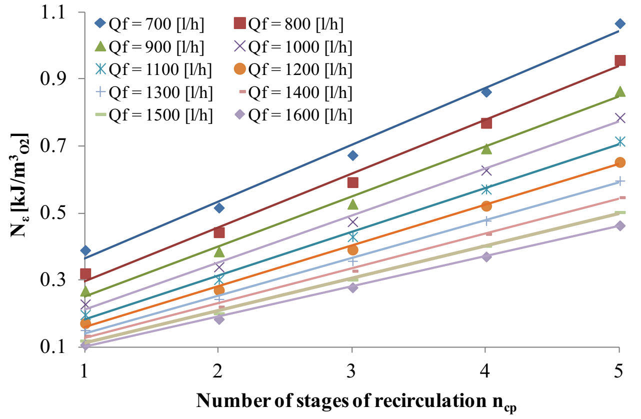

Fig. 11. Energy efficiency of the separation in the separator including permeate recirculation, as a function of feed flow and number of permeate recirculation cycles.

the initial pressure drop and to approach more favorable operational parameters. The highest individual value for the energy efficiency of separation has been reached for the lowest feed flow Q_f case (equal to Q_f = 800 dm³/h) in the retentate recirculation configuration. For this case, the value of N_ε was greater than 25%, when compared with the energy efficiency of the serial membrane connections configuration of the same volumetric feed flow. A brief summarization of values for the essential parameters, obtained for respective cases, are shown in Table 1.

The linear shape of the indicated characteristic curves for energy demand, comes primarily from the linear dependence of elementary energy consumption for the investigated unit with the feed flow. Since the gas compressors state the only energy-consuming elements within the applied mathematical model, total demand directly depends on the stream flow passing through the system. Although this assumption may decrease real consumption by neglecting energy required for auxiliary services (as valves control), it introduces the representative quantity for the purpose of comparative analysis. Nevertheless, the linearity of the curves in realized systems – may be partially biased by varying density of the fluid – caused by both a significant change in its composition and the variable energy efficiency of the compressor. The last of the mentioned factors might introduce crucial changes in the characteristic curves, especially in the case of invariable speed drive machines, fitted at different points of the system. Such to reduce potential influence of stated factors on final results, limited number of modules and the recirculation stages were concerned within the presented research. To perform an extended analysis, concerning investigation of membrane modules that contain a greater number of modules and/or recirculation stages, the current model should benefit from the implementation of a specific compressor characteristic datasheets.

4. Conclusions

The analysis concerning the energy consumption and energy-related separation parameters of the membrane separator is based upon a commercial capillary polymer membrane with varying connection schemes to the respective elements of the separator.

As the results indicate, the lowest energy demand for enrichment of the permeate, with 1 m³ of the oxygen, was obtained for a series type connection of modules and permeate recirculation, at greater feed flow rates. Nevertheless, the energy efficiency of the separation process does not depend on the number of interconnected membranes, in contrast to the number of permeate recirculation stages. Therefore, when considering a wide range of possible separator configurations for industrial processes, serial connection of the modules seems to be preferred. Furthermore, the useful energy ratio H – investigated for the serial connection of modules – power demand of the compressors corresponds to roughly a quarter of thermal energy input, which might potentially be extracted from gas coolers. If that heat could be introduced as a waste heat source for municipal hot water production or other useful energy generation, the energy demand for the compressors could be assumed as negligible. However, if this waste heat cannot be extracted, application of the serial connection will require additional expenditure,

Table 1
Summarized results for the computational analysis

Parameter	Serial connection of modules		Retentate recirculation		Permeate recirculation	
	Min.	Max.	Min.	Max.	Min.	Max.
N_{el}, kW	0.05	0.09	0.03	0.06	0.09	0.20
N_ε, kJ/m³ O_2	0.14	1.29	0.12	1.61	0.46	1.07

required for the maintenance of efficient cooling systems. Due to greater energy consumption, the application of the retentate recirculation configuration in the industrial membrane separators might be deemed as negligible.

Nevertheless, to follow increasing flexibility of units, as well as to prepare these systems to future modification, profound research in the operational parameters and energy consumption of mixed-connection separators should, therefore, be performed. Such investigation is an important matter for further research.

Acknowledgments

The research has been financially supported by the Silesian University of Technology by statutory research funds within the framework of the project no.: 08/050/BK_20/0209.

References

[1] G. Wiciak, J. Kotowicz, Experimental stand for CO_2 membrane separation, J. Power Technol., 91 (2011) 171–178.
[2] K.Q. Jiang, H. Yu, L.H. Chen, M.X. Fang, M. Azzi, A. Cottrell, K.K. Li, An advanced, ammonia-based combined NO_x/SO_x/CO_2 emission control process towards a low-cost, clean coal technology, Appl. Energy, 260 (2020) 114316, https://doi.org/10.1016/j.apenergy.2019.114316.
[3] O. Molchanov, K. Krpec, J. Horák, Electrostatic precipitation as a method to control the emissions of particulate matter from small-scale combustion units, J. Cleaner Prod., 246 (2020) 119022, https://doi.org/10.1016/j.jclepro.2019.119022.
[4] Z. Zhang, Q. Zeng, R.L. Hao, H.Z. He, F. Yang, X.Z. Mao, Y.M. Mao, P. Zhao, Combustion behavior, emission characteristics of SO_2, SO_3 and NO, and *in-situ* control of SO_2 and NO during the co-combustion of anthracite and dried sawdust sludge, Sci. Total Environ., 646 (2019) 716–726.
[5] A. Dryjańska, K. Janusz-Szymańska, The analysis of economic efficiency of oxy-type power plant on supercritical parameters with a capacity of 600 MW, Archivum Combustionis, 33 (2013) 109–123.
[6] M.E. Munawer, Human health and environmental impacts of coal combustion and post-combustion wastes, J. Sustainable Min., 17 (2018) 87–96.
[7] A. Mukherjee, J.A. Okolie, A. Abdelrasoul, C. Niu, A.K. Dalai, Review of post-combustion carbon dioxide capture technologies using activated carbon, J. Environ. Sci., 86 (2019) 46–63.
[8] Y. Yamauchi, K. Akiyama, Innovative zero-emission coal gasification power generation project, Energy Procedia, 37 (2013) 6579–6586.
[9] G. Verkhivker, E. Yantovski, Zero-emissions gas-fired cogeneration of power and hydrogen, Int. J. Hydrogen Energy, 26 (2001) 1109–1113.
[10] G.D. Surywanshi, B.B.K. Pillai, V.S. Patnaikuni, R. Vooradi, S.B. Anne, 4-E analyses of chemical looping combustion based subcritical, supercritical and ultra-supercritical coal-fired power plants, Energy Convers. Manage., 200 (2019) 112050, https://doi.org/10.1016/j.enconman.2019.112050.
[11] A. Skorek-Osikowska, Ł. Bartela, J. Kotowicz, Thermodynamic and ecological assessment of selected coal-fired power plants integrated with carbon dioxide capture, Appl. Energy, 200 (2017) 73–88.
[12] W. Stanek, L. Czarnowska, K. Pikoń, M. Bogacka, Thermodynamic and ecological assessment of selected coal-fired power plants integrated with carbon dioxide capture, Energy, 92 (2015) 341–348.
[13] S. Belošević, I. Tomanović, V. Beljanski, D. Tucaković, T. Živanović, Numerical prediction of processes for clean and efficient combustion of pulverized coal in power plants, Appl. Therm. Eng., 74 (2015) 102–110.
[14] V. Prabu, Integration of *in-situ* CO_2-oxy coal gasification with advanced power generating systems performing in a chemical looping approach of clean combustion, Appl. Energy, 140 (2015) 1–13.
[15] M. Harasimowicz, P. Orluk, G. Zakrzewska-Trznadel, A.G. Chmielewski, Application of polyimide membranes for biogas purification and enrichment, J. Hazard. Mater., 144 (2007) 698–702.
[16] G. Wiciak, Identification of select characteristics of separation CO_2 of the capillary polymer membrane, [Identyfikacja wybranych charakterystyk separacji CO_2 membrany kapilarnej polimerowej], Rynek Energii, 100 (2012) 94–100 (in Polish).
[17] J. Swolkień, Polish underground coal mines as point sources of methane emission to the atmosphere, Int. J. Greenhouse Gas Control, 94 (2020) 102921, https://doi.org/10.1016/j.ijggc.2019.102921.
[18] M. Rahman, M. Farhad Howladar, A. Hossain, A.T.M. Shahidul Huqe Muzemder, A. Al Numanbakth, Impact assessment of anthropogenic activities on water environment of Tillai River and its surroundings, Barapukuria Thermal Power Plant, Dinajpur, Bangladesh, Groundwater Sustainable Dev., 10 (2020) 100310, https://doi.org/10.1016/j.gsd.2019.100310.
[19] T. Trainer, Some problems in storing renewable energy, Energy Policy, 110 (2017) 386–393.
[20] M. Diesendorf, B. Elliston, The feasibility of 100% renewable electricity systems: a response to critics, Renewable Sustainable Energy Rev., 93 (2018) 318–330.
[21] S.Y. Chang, J.K. Zhuo, S. Meng, S.Y. Qin, Q. Yao, Clean coal technologies in china: current status and future perspectives, Engineering, 2 (2016) 447–459.
[22] J. Meyer, J. Mastin, T.-K. Bjørnebøle, T. Ryberg, N. Eldrup, Techno-economical study of the zero emission gas power concept, Energy Procedia, 4 (2011) 1949–1956.
[23] H. Nami, F. Ranjbar, M. Yari, Thermodynamic assessment of zero-emission power, hydrogen and methanol production using captured CO_2 from S-Graz oxy-fuel cycle and renewable hydrogen, Energy Convers. Manage., 161 (2018) 53–65.
[24] L. Remiorz, G. Wiciak, K. Grzywnowicz, Investigation of Applicability of Polyimide Membranes for Air Separation in Oxy-MILD Zero-Emission Power Plants, XXIV Research and Development in Power Engineering Conference, E3S Web of Conferences, Warsaw, 137 (2019) 01033.
[25] T. Chmielniak, H. Łukowicz, Condensing power plant cycle — assessing possibilities of improving its efficiency, Arch. Thermodyn., 31 (2010) 105–113.
[26] W. Chen, L. van der Ham, A. Nijmeijer, L. Winnubst, Membrane-integrated oxy-fuel combustion of coal: process design and simulation, J. Membr. Sci., 492 (2015) 461–470.
[27] S. Saeidi, S.M.S. Mahmoudi, H. Nami, M. Yari, Energy and exergy analyses of a novel near zero emission plant: combination of MATIANT cycle with gasification unit, Appl. Therm. Eng., 108 (2016) 893–904.
[28] M. Czyperek, P. Zapp, H.J.M. Bouwmeester, M. Modigell, K.-V. Peinemann, I. Voigt, W.A. Meulenberg, L. Singheiser, D. Stöver, MEM-BRAIN gas separation membranes for zero-emission fossil power plants, Energy Procedia, 1 (2009) 303–310.
[29] M. Rezakazemi, M. Sadrzadeh, T. Matsuura, Thermally stable polymers for advanced high-performance gas separation membranes, Prog. Energy Combust. Sci., 66 (2018) 1–41.
[30] C.A. Scholes, G.W. Stevens, S.E. Kentish, Membrane gas separation applications in natural gas processing, Fuel, 96 (2012) 15–28.
[31] D.M. Zhang, H.Z. Wang, C.X. Li, H. Meng, Modeling of purge-gas recovery using membrane separation, Chem. Eng. Res. Des., 125 (2017) 361–366.
[32] T. Banaszkiewicz, M. Chorowski, W. Gizicki, Comparative analysis of oxygen production for oxy-combustion application, Energy Procedia, 51 (2014) 127–134.
[33] A. Iulianelli, E. Drioli, Membrane engineering: latest advancements in gas separation and pre-treatment processes, petrochemical industry and refinery, and future perspectives in emerging applications, Fuel Process. Technol., 206 (2020) 106464, https://doi.org/10.1016/j.fuproc.2020.106464.

[34] M.B. Toftegaard, J. Brix, P.A. Jensen, P. Glarborg, A.D. Jensen, Oxy-fuel combustion of solid fuels, Prog. Energy Combust. Sci., 36 (2010) 581–625.
[35] K.K. Chen, W. Salim, Y. Han, D.Z. Wu, W.S.W. Ho, Fabrication and scale-up of multi-leaf spiral-wound membrane modules for CO_2 capture from flue gas, J. Membr. Sci., 595 (2020) 117504, https://doi.org/10.1016/j.memsci.2019.117504.
[36] Y. Han, W. Salim, K.K. Chen, D.Z. Wu, W.S.W. Ho, Field trial of spiral-wound facilitated transport membrane module for CO_2 capture from flue gas, J. Membr. Sci., 575 (2019) 242–251.
[37] S.H. Lee, S.K. Yun, J.-K. Kim, Development of novel sub-ambient membrane systems for energy-efficient post-combustion CO_2 capture, Appl. Energy, 238 (2019) 1060–1073.
[38] G. Wiciak, The influence of the moisture content in gaseous CO_2/N_2 mixture on selected parameters of CO_2 separation in a capillary polymeric membrane, Desal. Water Treat., 128 (2018) 314–323.
[39] R. Bounaceur, E. Berger, M. Pfister, A.A.R. Santos, E. Favre, Rigorous variable permeability modelling and process simulation for the design of polymeric membrane gas separation units: MEMSIC simulation tool, J. Membr. Sci., 523 (2017) 77–91.